# Search for charged Higgs bosons at LEP 2

P. Abreu, W. Adam, T. Adye, P. Adzic, Z. Albrecht, T. Alderweireld, G.D. Alekseev, R. Alemany, T. Allmendinger, P.P. Allport, et al.

EUROPEAN ORGANIZATION FOR NUCLEAR RESEARCH

CERN–EP/99–77

4 June 1999

# Search for Charged Higgs Bosons at LEP 2

DELPHI Collaboration

**Abstract**

A search for pair produced charged Higgs bosons has been performed in the high energy data collected by DELPHI at LEP with $\sqrt{s}$ = 161, 172 and 183 GeV. The analysis uses the $\tau\nu\tau\nu$, $c\bar{s}\tau\nu$ and $c\bar{s}\bar{c}s$ final states and a combination of event shape variables, di-jet masses and jet flavour tagging for the separation of a possible signal from the dominant $W^+W^-$ and QCD backgrounds. The number of selected events has been found to be compatible with the expected background. The lower excluded value of the $H^\pm$ mass obtained by varying the $H^\pm \to$ hadrons decay branching ratio has been found to be 56.3 GeV/$c^2$.

(Accepted by Phys. Lett. B)

P.Abreu[21], W.Adam[50], T.Adye[36], P.Adzic[11], Z.Albrecht[17], T.Alderweireld[2], G.D.Alekseev[16], R.Alemany[49], T.Allmendinger[17], P.P.Allport[22], S.Almehed[24], U.Amaldi[9], N.Amapane[45], S.Amato[47], E.G.Anassontzis[3], P.Andersson[44], A.Andreazza[9], S.Andringa[21], P.Antilogus[25], W-D.Apel[17], Y.Arnoud[9], B.Åsman[44], J-E.Augustin[25], A.Augustinus[9], P.Baillon[9], P.Bambade[19], F.Barao[21], G.Barbiellini[46], R.Barbier[25], D.Y.Bardin[16], G.Barker[17], A.Baroncelli[38], M.Battaglia[15], M.Baubillier[23], K-H.Becks[52], M.Begalli[6], A.Behrmann[52], P.Beilliere[8], Yu.Belokopytov[9,53], K.Belous[42], N.C.Benekos[31], A.C.Benvenuti[5], C.Berat[14], M.Berggren[25], D.Bertini[25], D.Bertrand[2], M.Besancon[39], M.Bigi[45], M.S.Bilenky[16], M-A.Bizouard[19], D.Bloch[10], H.M.Blom[30], M.Bonesini[27], W.Bonivento[27], M.Boonekamp[39], P.S.L.Booth[22], A.W.Borgland[4], G.Borisov[19], C.Bosio[41], O.Botner[48], E.Boudinov[30], B.Bouquet[19], C.Bourdarios[19], T.J.V.Bowcock[22], I.Boyko[16], I.Bozovic[11], M.Bozzo[13], P.Branchini[38], T.Brenke[52], R.A.Brenner[48], P.Bruckman[18], J-M.Brunet[8], L.Bugge[32], T.Buran[32], T.Burgsmueller[52], B.Buschbeck[50], P.Buschmann[52], S.Cabrera[49], M.Caccia[27], M.Calvi[27], T.Camporesi[9], V.Canale[37], F.Carena[9], L.Carroll[22], C.Caso[13], M.V.Castillo Gimenez[49], A.Cattai[9], F.R.Cavallo[5], V.Chabaud[9], M.Chapkin[42], Ph.Charpentier[9], L.Chaussard[25], P.Checchia[35], G.A.Chelkov[16], R.Chierici[45], P.Chliapnikov[42], P.Chochula[7], V.Chorowicz[25], J.Chudoba[29], K.Cieslik[18], P.Collins[9], R.Contri[13], E.Cortina[49], G.Cosme[19], F.Cossutti[9], J-H.Cowell[22], H.B.Crawley[1], D.Crennell[36], S.Crepe[14], G.Crosetti[13], J.Cuevas Maestro[33], S.Czellar[15], M.Davenport[9], W.Da Silva[23], A.Deghorain[2], G.Della Ricca[46], P.Delpierre[26], N.Demaria[9], A.De Angelis[9], W.De Boer[17], C.De Clercq[2], B.De Lotto[46], A.De Min[35], L.De Paula[47], H.Dijkstra[9], L.Di Ciaccio[37,9], J.Dolbeau[8], K.Doroba[51], M.Dracos[10], J.Drees[52], M.Dris[31], A.Duperrin[25], J-D.Durand[9], G.Eigen[4], T.Ekelof[48], G.Ekspong[44], M.Ellert[48], M.Elsing[9], J-P.Engel[10], B.Erzen[43], M.Espirito Santo[21], G.Fanourakis[11], D.Fassouliotis[11], J.Fayot[23], M.Feindt[17], A.Fenyuk[42], P.Ferrari[27], A.Ferrer[49], E.Ferrer-Ribas[19], F.Ferro[13], S.Fichet[23], A.Firestone[1], U.Flagmeyer[52], H.Foeth[9], E.Fokitis[31], F.Fontanelli[13], B.Franek[36], A.G.Frodesen[4], R.Fruhwirth[50], F.Fulda-Quenzer[19], J.Fuster[49], A.Galloni[22], D.Gamba[45], S.Gamblin[19], M.Gandelman[47], C.Garcia[49], C.Gaspar[9], M.Gaspar[47], U.Gasparini[35], Ph.Gavillet[9], E.N.Gazis[31], D.Gele[10], N.Ghodbane[25], I.Gil[49], F.Glege[52], R.Gokieli[9,51], B.Golob[43], G.Gomez-Ceballos[40], P.Goncalves[21], I.Gonzalez Caballero[40], G.Gopal[36], L.Gorn[1,54], Yu.Gouz[42], V.Gracco[13], J.Grahl[1], E.Graziani[38], C.Green[22], H-J.Grimm[17], P.Gris[39], G.Grosdidier[19], K.Grzelak[51], M.Gunther[48], J.Guy[36], F.Hahn[9], S.Hahn[52], S.Haider[9], A.Hallgren[48], K.Hamacher[52], J.Hansen[32], F.J.Harris[34], V.Hedberg[24], S.Heising[17], J.J.Hernandez[49], P.Herquet[2], H.Herr[9], T.L.Hessing[34], J.-M.Heuser[52], E.Higon[49], S-O.Holmgren[44], P.J.Holt[34], S.Hoorelbeke[2], M.Houlden[22], J.Hrubec[50], K.Huet[2], G.J.Hughes[22], K.Hultqvist[44], J.N.Jackson[22], R.Jacobsson[9], P.Jalocha[9], R.Janik[7], Ch.Jarlskog[24], G.Jarlskog[24], P.Jarry[39], B.Jean-Marie[19], E.K.Johansson[44], P.Jonsson[25], C.Joram[9], P.Juillot[10], F.Kapusta[23], K.Karafasoulis[11], S.Katsanevas[25], E.C.Katsoufis[31], R.Keranen[17], B.P.Kersevan[43], B.A.Khomenko[16], N.N.Khovanski[16], A.Kiiskinen[15], B.King[22], A.Kinvig[22], N.J.Kjaer[30], O.Klapp[52], H.Klein[9], P.Kluit[30], P.Kokkinias[11], M.Koratzinos[9], V.Kostioukhine[42], C.Kourkoumelis[3], O.Kouznetsov[39], M.Krammer[50], E.Kriznic[43], P.Krstic[11], Z.Krumstein[16], P.Kubinec[7], J.Kurowska[51], K.Kurvinen[15], J.W.Lamsa[1], D.W.Lane[1], P.Langefeld[52], V.Lapin[42], J-P.Laugier[39], R.Lauhakangas[15], G.Leder[50], F.Ledroit[14], V.Lefebure[2], L.Leinonen[44], A.Leisos[11], R.Leitner[29], G.Lenzen[52], V.Lepeltier[19], T.Lesiak[18], M.Lethuillier[39], J.Libby[34], D.Liko[9], A.Lipniacka[44], I.Lippi[35], B.Loerstad[24], J.G.Loken[34], J.H.Lopes[47], J.M.Lopez[40], R.Lopez-Fernandez[14], D.Loukas[11], P.Lutz[39], L.Lyons[34], J.MacNaughton[50], J.R.Mahon[6], A.Maio[21], A.Malek[52], T.G.M.Malmgren[44], S.Maltezos[31], V.Malychev[16], J.Marco[40], R.Marco[40], B.Marechal[47], M.Margoni[35], J-C.Marin[9], C.Mariotti[9], A.Markou[11], C.Martinez-Rivero[19], F.Martinez-Vidal[49], S.Marti i Garcia[9], J.Masik[12], N.Mastroyiannopoulos[11], F.Matorras[40], C.Matteuzzi[27], G.Matthiae[37], F.Mazzucato[35], M.Mazzucato[35], M.Mc Cubbin[22], R.Mc Kay[1], R.Mc Nulty[22], G.Mc Pherson[22], C.Meroni[27], W.T.Meyer[1], E.Migliore[45], L.Mirabito[25], W.A.Mitaroff[50], U.Mjoernmark[24], T.Moa[44], M.Moch[17], R.Moeller[28], K.Moenig[9], M.R.Monge[13], X.Moreau[23], P.Morettini[13], G.Morton[34], U.Mueller[52], K.Muenich[52], M.Mulders[30], C.Mulet-Marquis[14], R.Muresan[24], W.J.Murray[36], B.Muryn[14,18], G.Myatt[34], T.Myklebust[32], F.Naraghi[14], M.Nassiakou[11], F.L.Navarria[5], S.Navas[49], K.Nawrocki[51], P.Negri[27], S.Nemecek[12], N.Neufeld[9], R.Nicolaidou[39], B.S.Nielsen[28], P.Niezurawski[51], M.Nikolenko[10,16], V.Nomokonov[15], A.Normand[22], A.Nygren[24], V.Obraztsov[42], A.G.Olshevski[16], A.Onofre[21], R.Orava[15], G.Orazi[10], K.Osterberg[15], A.Ouraou[39], M.Paganoni[27], S.Paiano[5], R.Pain[23], R.Paiva[21], J.Palacios[34], H.Palka[18], Th.D.Papadopoulou[31,9], K.Papageorgiou[11], L.Pape[9], C.Parkes[9], F.Parodi[13], U.Parzefall[22], A.Passeri[38], O.Passon[52], M.Pegoraro[35], L.Peralta[21], M.Pernicka[50], A.Perrotta[5], C.Petridou[46], A.Petrolini[13], H.T.Phillips[36], F.Pierre[39], M.Pimenta[21], E.Piotto[27], T.Podobnik[43], M.E.Pol[6], G.Polok[18], P.Poropat[46], V.Pozdniakov[16], P.Privitera[37], N.Pukhaeva[16], A.Pullia[27], D.Radojicic[34], S.Ragazzi[27], H.Rahmani[31], P.N.Ratoff[20], A.L.Read[32], P.Rebecchi[9], N.G.Redaelli[27], M.Regler[50], D.Reid[30], R.Reinhardt[52], P.B.Renton[34], L.K.Resvanis[3], F.Richard[19], J.Ridky[12], G.Rinaudo[45], O.Rohne[32], A.Romero[45], P.Ronchese[35], E.I.Rosenberg[1], P.Rosinsky[7], P.Roudeau[19], T.Rovelli[5], Ch.Royon[39], V.Ruhlmann-Kleider[39], A.Ruiz[40], H.Saarikko[15], Y.Sacquin[39], A.Sadovsky[16], G.Sajot[14], J.Salt[49], D.Sampsonidis[11], M.Sannino[13], H.Schneider[17], Ph.Schwemling[23], B.Schwering[52], U.Schwickerath[17], M.A.E.Schyns[52], F.Scuri[46], P.Seager[20], Y.Sedykh[16], A.M.Segar[34], R.Sekulin[36], R.C.Shellard[6], A.Sheridan[22], M.Siebel[52], L.Simard[39], F.Simonetto[35], A.N.Sisakian[16],

G.Smadja[25], O.Smirnova[24], G.R.Smith[36], A.Sokolov[42], A.Sopczak[17], R.Sosnowski[51], T.Spassov[21], E.Spiriti[38], P.Sponholz[52], S.Squarcia[13], C.Stanescu[38], S.Stanic[43], K.Stevenson[34], A.Stocchi[19], J.Strauss[50], R.Strub[10], B.Stugu[4], M.Szczekowski[51], M.Szeptycka[51], T.Tabarelli[27], F.Tegenfeldt[48], F.Terranova[27], J.Thomas[34], J.Timmermans[30], N.Tinti[5], L.G.Tkatchev[16], S.Todorova[10], A.Tomaradze[2], B.Tome[21], A.Tonazzo[9], L.Tortora[38], G.Transtromer[24], D.Treille[9], G.Tristram[8], M.Trochimczuk[51], C.Troncon[27], A.Tsirou[9], M-L.Turluer[39], I.A.Tyapkin[16], S.Tzamarias[11], O.Ullaland[9], V.Uvarov[42], G.Valenti[5], E.Vallazza[46], G.W.Van Apeldoorn[30], P.Van Dam[30], W.K.Van Doninck[2], J.Van Eldik[30], A.Van Lysebetten[2], N.Van Remortel[2], I.Van Vulpen[30], N.Vassilopoulos[34], G.Vegni[27], L.Ventura[35], W.Venus[36,9], F.Verbeure[2], M.Verlato[35], L.S.Vertogradov[16], V.Verzi[37], D.Vilanova[39], L.Vitale[46], E.Vlasov[42], A.S.Vodopyanov[16], C.Vollmer[17], G.Voulgaris[3], V.Vrba[12], H.Wahlen[52], C.Walck[44], C.Weiser[17], D.Wicke[52], J.H.Wickens[2], G.R.Wilkinson[9], M.Winter[10], M.Witek[18],

G.Wolf[9], J.Yi[1], O.Yushchenko[42], A.Zaitsev[42], A.Zalewska[18], P.Zalewski[51], D.Zavrtanik[43], E.Zevgolatakos[11], N.I.Zimin[16,24], G.C.Zucchelli[44], G.Zumerle[35]

[1]Department of Physics and Astronomy, Iowa State University, Ames IA 50011-3160, USA
[2]Physics Department, Univ. Instelling Antwerpen, Universiteitsplein 1, BE-2610 Wilrijk, Belgium
and IIHE, ULB-VUB, Pleinlaan 2, BE-1050 Brussels, Belgium
and Faculté des Sciences, Univ. de l'Etat Mons, Av. Maistriau 19, BE-7000 Mons, Belgium
[3]Physics Laboratory, University of Athens, Solonos Str. 104, GR-10680 Athens, Greece
[4]Department of Physics, University of Bergen, Allégaten 55, NO-5007 Bergen, Norway
[5]Dipartimento di Fisica, Università di Bologna and INFN, Via Irnerio 46, IT-40126 Bologna, Italy
[6]Centro Brasileiro de Pesquisas Físicas, rua Xavier Sigaud 150, BR-22290 Rio de Janeiro, Brazil
and Depto. de Física, Pont. Univ. Católica, C.P. 38071 BR-22453 Rio de Janeiro, Brazil
and Inst. de Física, Univ. Estadual do Rio de Janeiro, rua São Francisco Xavier 524, Rio de Janeiro, Brazil
[7]Comenius University, Faculty of Mathematics and Physics, Mlynska Dolina, SK-84215 Bratislava, Slovakia
[8]Collège de France, Lab. de Physique Corpusculaire, IN2P3-CNRS, FR-75231 Paris Cedex 05, France
[9]CERN, CH-1211 Geneva 23, Switzerland
[10]Institut de Recherches Subatomiques, IN2P3 - CNRS/ULP - BP20, FR-67037 Strasbourg Cedex, France
[11]Institute of Nuclear Physics, N.C.S.R. Demokritos, P.O. Box 60228, GR-15310 Athens, Greece
[12]FZU, Inst. of Phys. of the C.A.S. High Energy Physics Division, Na Slovance 2, CZ-180 40, Praha 8, Czech Republic
[13]Dipartimento di Fisica, Università di Genova and INFN, Via Dodecaneso 33, IT-16146 Genova, Italy
[14]Institut des Sciences Nucléaires, IN2P3-CNRS, Université de Grenoble 1, FR-38026 Grenoble Cedex, France
[15]Helsinki Institute of Physics, HIP, P.O. Box 9, FI-00014 Helsinki, Finland
[16]Joint Institute for Nuclear Research, Dubna, Head Post Office, P.O. Box 79, RU-101 000 Moscow, Russian Federation
[17]Institut für Experimentelle Kernphysik, Universität Karlsruhe, Postfach 6980, DE-76128 Karlsruhe, Germany
[18]Institute of Nuclear Physics and University of Mining and Metalurgy, Ul. Kawiory 26a, PL-30055 Krakow, Poland
[19]Université de Paris-Sud, Lab. de l'Accélérateur Linéaire, IN2P3-CNRS, Bât. 200, FR-91405 Orsay Cedex, France
[20]School of Physics and Chemistry, University of Lancaster, Lancaster LA1 4YB, UK
[21]LIP, IST, FCUL - Av. Elias Garcia, 14-1$^o$, PT-1000 Lisboa Codex, Portugal
[22]Department of Physics, University of Liverpool, P.O. Box 147, Liverpool L69 3BX, UK
[23]LPNHE, IN2P3-CNRS, Univ. Paris VI et VII, Tour 33 (RdC), 4 place Jussieu, FR-75252 Paris Cedex 05, France
[24]Department of Physics, University of Lund, Sölvegatan 14, SE-223 63 Lund, Sweden
[25]Université Claude Bernard de Lyon, IPNL, IN2P3-CNRS, FR-69622 Villeurbanne Cedex, France
[26]Univ. d'Aix - Marseille II - CPP, IN2P3-CNRS, FR-13288 Marseille Cedex 09, France
[27]Dipartimento di Fisica, Università di Milano and INFN, Via Celoria 16, IT-20133 Milan, Italy
[28]Niels Bohr Institute, Blegdamsvej 17, DK-2100 Copenhagen Ø, Denmark
[29]NC, Nuclear Centre of MFF, Charles University, Areal MFF, V Holesovickach 2, CZ-180 00, Praha 8, Czech Republic
[30]NIKHEF, Postbus 41882, NL-1009 DB Amsterdam, The Netherlands
[31]National Technical University, Physics Department, Zografou Campus, GR-15773 Athens, Greece
[32]Physics Department, University of Oslo, Blindern, NO-1000 Oslo 3, Norway
[33]Dpto. Fisica, Univ. Oviedo, Avda. Calvo Sotelo s/n, ES-33007 Oviedo, Spain
[34]Department of Physics, University of Oxford, Keble Road, Oxford OX1 3RH, UK
[35]Dipartimento di Fisica, Università di Padova and INFN, Via Marzolo 8, IT-35131 Padua, Italy
[36]Rutherford Appleton Laboratory, Chilton, Didcot OX11 OQX, UK
[37]Dipartimento di Fisica, Università di Roma II and INFN, Tor Vergata, IT-00173 Rome, Italy
[38]Dipartimento di Fisica, Università di Roma III and INFN, Via della Vasca Navale 84, IT-00146 Rome, Italy
[39]DAPNIA/Service de Physique des Particules, CEA-Saclay, FR-91191 Gif-sur-Yvette Cedex, France
[40]Instituto de Fisica de Cantabria (CSIC-UC), Avda. los Castros s/n, ES-39006 Santander, Spain
[41]Dipartimento di Fisica, Università degli Studi di Roma La Sapienza, Piazzale Aldo Moro 2, IT-00185 Rome, Italy
[42]Inst. for High Energy Physics, Serpukov P.O. Box 35, Protvino, (Moscow Region), Russian Federation
[43]J. Stefan Institute, Jamova 39, SI-1000 Ljubljana, Slovenia and Laboratory for Astroparticle Physics,
Nova Gorica Polytechnic, Kostanjeviska 16a, SI-5000 Nova Gorica, Slovenia,
and Department of Physics, University of Ljubljana, SI-1000 Ljubljana, Slovenia
[44]Fysikum, Stockholm University, Box 6730, SE-113 85 Stockholm, Sweden
[45]Dipartimento di Fisica Sperimentale, Università di Torino and INFN, Via P. Giuria 1, IT-10125 Turin, Italy
[46]Dipartimento di Fisica, Università di Trieste and INFN, Via A. Valerio 2, IT-34127 Trieste, Italy
and Istituto di Fisica, Università di Udine, IT-33100 Udine, Italy
[47]Univ. Federal do Rio de Janeiro, C.P. 68528 Cidade Univ., Ilha do Fundão BR-21945-970 Rio de Janeiro, Brazil
[48]Department of Radiation Sciences, University of Uppsala, P.O. Box 535, SE-751 21 Uppsala, Sweden
[49]IFIC, Valencia-CSIC, and D.F.A.M.N., U. de Valencia, Avda. Dr. Moliner 50, ES-46100 Burjassot (Valencia), Spain
[50]Institut für Hochenergiephysik, Österr. Akad. d. Wissensch., Nikolsdorfergasse 18, AT-1050 Vienna, Austria
[51]Inst. Nuclear Studies and University of Warsaw, Ul. Hoza 69, PL-00681 Warsaw, Poland
[52]Fachbereich Physik, University of Wuppertal, Postfach 100 127, DE-42097 Wuppertal, Germany
[53]On leave of absence from IHEP Serpukhov
[54]Now at University of Florida

# 1 Introduction

The existence of a charged Higgs boson doublet is predicted by several extensions of the Standard Model and in particular by Supersymmetry. At LEP 2, charged Higgs bosons can be produced in pairs and decay predominantly in either $\tau\bar{\nu}$ or $c\bar{s}$ final states [1]. A search for pair-produced charged Higgs bosons has been performed based on the data collected by DELPHI during the LEP runs at centre-of-mass energies $\sqrt{s}$ of 161 GeV, 172 GeV and 183 GeV. The results reported in this paper supersede those obtained in an earlier analysis of the DELPHI data limited to the 161 GeV and 172 GeV runs [1]. Similar searches have been performed by the other LEP experiments [2]. As the higher centre-of-mass energy gives sensitivity to Higgs masses closer to that of the W boson, the background from $e^+e^- \rightarrow \mathrm{W}^+\mathrm{W}^-$ becomes more important. The cross-section for $\mathrm{W}^\pm$ production is two orders of magnitude higher than that predicted for $\mathrm{H}^\pm$ of equal mass, therefore searches are significantly less sensitive to Higgs mass values close to the $\mathrm{W}^\pm$ mass peak. In order to retain sensitivity to the possible signal from charged Higgs boson decays, effective rejection of this background is very important. A new technique has been developed to improve the discrimination against the hadronic W decays in the search for $\mathrm{H}^\pm$ candidates. In section 2 the event reconstruction and the definition of the discriminating variables are discussed separately for the hadronic, semileptonic and fully leptonic final states with particular emphasis on the $\sqrt{s} = 183$ GeV data. Section 3 describes the results from the combined DELPHI data at LEP 2.

# 2 Data Analysis

The analysis has been performed on the data collected by the DELPHI detector at LEP 2 at centre-of-mass energies of 161 GeV, 172 GeV and 183 GeV. The DELPHI detector and its performance have already been described in detail elsewhere [3,4]. The corresponding integrated luminosities are 9.95 pb$^{-1}$, 10.16 pb$^{-1}$ and 53.5 pb$^{-1}$ respectively.

Charged particle tracks have been required to satisfy the following quality criteria. Only particles with momentum larger than 100 MeV/$c$, relative momentum error $\Delta\, p/p < 1$ and track length larger than 30 cm have been used. In addition, the impact parameter to the event primary vertex had to be smaller than 4.0 cm in the projection on the plane normal to the beam axis and smaller than 10.0 cm along the beam axis. Kaons have been identified by the combined response of the RICH detectors and the specific ionisation measured in the TPC [4,5]. Neutral particles have been required to have energy deposit larger than 200 MeV in the electromagnetic calorimeters or larger than 500 MeV in the hadron calorimeter.

$\mathrm{H}^+\mathrm{H}^-$ signal samples were produced with the PYTHIA generator [6] at four different $\mathrm{H}^\pm$ masses: 50 GeV/$c^2$, 55 GeV/$c^2$, 60 GeV/$c^2$ and 65 GeV/$c^2$. The $q\bar{q}\gamma$ QCD background sample was also produced using PYTHIA and the four fermion final states, including $\mathrm{W}^+\mathrm{W}^-$ and $\mathrm{Z}^0\mathrm{Z}^0$, were produced with the EXCALIBUR generator [7]. The main background contribution from four fermion processes is due to $\mathrm{W}^+\mathrm{W}^-$ pairs which are referred to as $\mathrm{W}^+\mathrm{W}^-$ in the rest of the paper. The VDM and QCD components of the two photon interactions leading to hadronic final states were generated using TWOGAM [8]. The generators of Berends, Daverveldt and Kleiss [9] were used for the QPM component and for leptonic final states. In addition, $\mathrm{Z}^0\mathrm{Z}^0$, $\mathrm{W}e\bar{\nu}$ and $\mathrm{Z}e^+e^-$ samples generated with

[1] Throughout the paper the charge-conjugate states are implicitly included

PYTHIA, $\mu^+\mu^-(\gamma)$ and $\tau^+\tau^-(\gamma)$ events generated with the KORALZ [10] generator have been used for the estimate of the background in the fully leptonic channel.

## 2.1 The hadronic channel

In the fully hadronic decay channel, each charged Higgs is expected to decay into a $c\bar{s}$ pair, producing a four jet final state.

The hadronic four jet event selection followed in this analysis is the same as for the DELPHI neutral Higgs analysis [11]. In addition, events with two or more jets tagged as containing $b$ quarks, by the jet flavour tagging algorithm described below, have also been removed. In order to reduce the amount of QCD background and of wrongly reconstructed $W^+W^-$ decays, only events with four reconstructed jets, using the LUCLUS algorithm [6] with $d_{join} = 6.5$ GeV/$c^2$, have been accepted.

Energy-momentum conservation has been imposed by performing a 4-C fit on these events and the difference between the two di-jet masses for each jet pairing has been computed. A 5-C fit, assuming equal boson masses, has been applied in order to improve the resolution on the di-jet mass $M_{jj}$. The di-jet combination giving the smallest $\chi^2$ has been selected for the mass reconstruction. Events for which the $\chi^2$ per degree of freedom of this combination exceeded 5 or the difference of the masses computed after the 4-C fit exceeded 8 GeV/$c^2$ have been rejected.

Only events with 40 GeV/$c^2 < M_{jj} <$ 70 GeV/$c^2$ have been considered for this analysis.

The two main sources of background in this channel are the $q\bar{q}gg$ QCD background and fully hadronic decays of $W^+W^-$ pairs. The charged Higgs boson is expected to couple predominantly to $c\bar{s}$ in its hadronic decay mode. Therefore the QCD and $W^+W^-$ backgrounds can be partially suppressed with regard to the signal by selecting final states consistent with being $c\bar{s}\bar{c}s$. A flavour tagging algorithm has been developed for the study of multiparton final states [12]. This tagging is based on the response of nine discriminating variables: three of them are related to the identified lepton and hadron content of the jet, two depend on kinematical variables and four on the reconstructed secondary decay structure. The finite $c$ lifetime is exploited to distinguish between $c$ and light quark jets, while the $c$ mass and decay multiplicity, smaller than for beauty quarks, was used to discriminate against $b$ jets. Further, $s$ and $c$ jets can be distinguished from $u$ and $d$ jets by the presence of an identified energetic kaon. A likelihood variable was computed from the response of the individual jet variables as discussed below for the anti-WW and anti-QCD functions. The responses for the individual jets were further combined into a global $c\bar{s}\bar{c}s$ event probability.

QCD background events differ also kinematically from pair-produced bosons [13]. In order to separate the signal from the QCD background the following variables have been used together with the $c\bar{s}\bar{c}s$ probability from the jet flavour tagging algorithm: the product of the minimum jet energy and the minimum di-jet angle, $\min(E_{jet}) \cdot \min(\alpha_{jets})$, the di-jet pair mass difference after 4-C fit and the polar angle of the thrust axis. These variables have been combined to form an event anti-QCD likelihood function separating QCD events from pair-produced bosons. The likelihood function has been defined as follows. For each of the $N$ discriminating variables, the fractions $F_i^{HH}(x_i)$ and $F_i^{QCD}(x_i)$ of respectively $H^+H^-$ and QCD events corresponding to a given value $x_i$ of the $i^{th}$ variable, have been extracted from a sample of simulated QCD and $H^+H^-$ events with equal populations. The anti-QCD likelihood has been computed as the normalised product of these individual fractions, $\prod_{i=1,N} F_i^{HH}(x_i)/(\prod_{i=1,N} F_i^{HH}(x_i) + \prod_{i=1,N} F_i^{QCD}(x_i))$. The response of this likelihood discriminates $H^+H^-$ events from the QCD background but not from

$W^+W^-$ events, due to the similarity in the kinematics for these two processes. Therefore other signatures have been used to distinguish possible signal events from $W^+W^-$ pairs and other four fermion background.

Correctly reconstructed events from on-shell $W^\pm \to q\bar{q}$ decays result in di-jet masses consistent with the W mass and are therefore above the mass region of interest for the present $H^\pm$ search. However, wrong di-jet pairing, decays of off-shell W bosons and events with incorrect jet reconstruction may result in an apparent boson mass below 70 GeV/$c^2$. A simulation study has shown that the wrong di-jet pairing is the dominant source of these backgrounds. Therefore all three possible jet pairings for a given event have been tested for the hypothesis to be either a correctly paired $W^+W^-$ or $H^+H^-$ event. Likelihoods have been computed for each pairing, using the $\chi^2$ from the 5-C fit, the difference between the reconstructed di-jet mass and the nominal W mass and the boson production polar angle, i.e. the polar angle of the di-jet momentum vector. A jet-pairing W tag variable has been defined as $L^W_{max}/(L^H_{max} + L^W_{max})$ where $L^{H,W}_{max}$ represents the largest of the three likelihoods for the H and W hypotheses respectively. This tag variable is peaked at zero in both $H^+H^-$ and QCD events while for the majority of the $W^+W^-$ events it is uniformly distributed between 0 and 1.

Table 1: *Number of selected events and signal efficiency in the hadronic final state at different stages of the event selection procedure for $\sqrt{s}$ = 183 GeV.*

| Selection | Data | Total Bkg | $W^+W^-$ Bkg | QCD Bkg | Efficiency $H^+H^-$ ($M_H$=60 GeV/$c^2$) |
|---|---|---|---|---|---|
| Event preselection | 544 | 548.0 ± 3.6 | 353.7 | 194.3 | 0.80 ± 0.01 |
| 4 Jets | 319 | 302.6 ± 2.0 | 218.2 | 84.4 | 0.52 ± 0.01 |
| $\chi^2$ Cut | 265 | 242.9 ± 1.8 | 183.1 | 59.8 | 0.45 ± 0.01 |
| $\Delta M$ Cut | 138 | 122.3 ± 1.6 | 98.9 | 23.4 | 0.32 ± 0.01 |
| $40 < M_{JJ} < 70$ | 34 | 32.3 ± 0.9 | 19.2 | 13.1 | 0.28 ± 0.01 |
| Probability Cuts | 11 | 11.8 ± 0.6 | 6.9 | 4.9 | 0.22 ± 0.01 |

Finally, normalised fractions of $H^+H^-$ signal events as a function of the polar angle of the event thrust axis, the di-jet mass difference and the jet pairing W tag variable have been combined with the probability from the jet flavour tagging algorithm into an event anti-WW likelihood using the same procedure as for the anti-QCD likelihood. The $Z^0Z^0$ production cross-section is small and the $Z^0$ mass is high enough to make the $Z^0Z^0$ background insignificant compared to QCD and $W^+W^-$ backgrounds at masses below 70 GeV/$c^2$.

Using the simulation, the cuts on the two likelihood variables have been optimised separately for each centre-of-mass energy following a procedure discussed in section 3 (see Figure 1). The number of real data events, expected backgrounds and the signal efficiency after each of the set of cuts adopted in the analysis are given in Table 1 for the highest energy sample.

## 2.2 The semileptonic channel

In this channel one of the charged Higgs bosons decays into a $c\bar{s}$ quark pair, while the other decays into $\tau\bar{\nu}$. Such an event is characterised by two hadronic jets, a $\tau$ candidate and missing energy carried by the neutrinos. The dominating background processes are $q\bar{q}\gamma$ and $q\bar{q}g$ events and semileptonic decays of $W^+W^-$.

Charged particles with momentum greater than 400 MeV/$c$ were used in this channel and at least eight were required for the preselected sample of events. Further, the energy in charged particles had to exceed 0.15 $\sqrt{s}$, and the total detected energy had to be greater than 0.30 $\sqrt{s}$. After a clustering into two jets using the DURHAM algorithm [14], the acollinearity had to be greater than 10°. Events were also required to have no neutral particles with energy above 30 GeV and the energy detected in a cone of 20° (30°) half aperture around the beam axis had to be less than 0.20 $\sqrt{s}$ (0.30 $\sqrt{s}$). Further, the angle between the total momentum of the detected particles in the event and the beam axis had to be greater than 20°. After clustering into three jets, the jet with the smallest charged particle multiplicity was treated as the $\tau$ candidate. In case more than one jet had the same number of charged particles, the least energetic jet was chosen.

$\tau$ jet candidates were required to have less than eight particles, of which less than four were charged. At least one of the tracks in this jet was required to have track elements in the Vertex Detector and the TPC and either energy deposit in the e.m. calorimeter or hits in the Outer Detector, the Forward Chambers or the Muon Chambers. In addition, the visible energy of the $\tau$ candidate had to be greater than 0.02 $\sqrt{s}$.

The mass of the decaying bosons, $M_{jj}$, was reconstructed using a constrained fit requiring energy and momentum conservation and equal mass of the decaying bosons. The three components of the momentum vector of the neutrino and the magnitude of the $\tau$ momentum have been treated as free parameters, reducing the number of degrees of freedom in the fit from 5 to 1. The $\tau$ lepton direction was approximated by that of the reconstructed jet. Only events with mass in the range 40 GeV/$c^2$ $< M_{jj} <$ 70 GeV/$c^2$ have been further considered in the analysis.

Likelihood functions for a given event to be a QCD or a $W^+W^-$ background event have then been defined similarly to the case of the hadronic channel described above. The polar angle of the total momentum, the logarithm of the clustering distance, defined as the $y_{cut}$ value in the DURHAM algorithm for which the number of jets changes from two to three, and the maximum angle between two particles from the $\tau$ candidate have been used as discriminating variables to define the event anti-QCD likelihood. For the event anti-WW likelihood the variables used were the reconstructed polar angle of the negatively charged boson (where the charge has been taken to be that of the leading charged particle from the $\tau$ decay), the visible $\tau$ energy, the angle between the two hadronic jets and the $c\bar{s}$ probability of the hadronic di-jet.

The cuts on the two likelihood variables have been optimised separately for the three $\sqrt{s}$ energies as discussed in section 3 (see Figure 2). The number of real data events, expected backgrounds and the signal efficiency after each of the set of cuts adopted in the analysis are given in Table 2 for the highest energy sample.

Table 2: *Number of selected events and signal efficiency in the semi-leptonic final state at different stages of the event selection procedure for $\sqrt{s}$ = 183 GeV.*

| Selection | Data | Total Bkg | $W^+W^-$ Bkg | QCD Bkg | Efficiency $H^+H^-$ ($M_H$=60 GeV/$c^2$) |
|---|---|---|---|---|---|
| Event Preselection | 354 | 332.3 ± 2.7 | 216.0 | 98.3 | 0.55 ± 0.02 |
| $\tau$ selection | 303 | 295.6 ± 2.6 | 205.0 | 74.8 | 0.52 ± 0.02 |
| $40 < M_{jj} < 70$ | 41 | 42.6 ± 1.1 | 21.8 | 15.7 | 0.39 ± 0.02 |
| Probability Cuts | 4 | 3.3 ± 0.3 | 2.5 | 0.5 | 0.31 ± 0.02 |

### 2.3 The leptonic channel

In this channel both charged Higgs bosons decay into a $\tau\bar{\nu}$ pair. These events are characterised by two acollinear slim jets and missing energy carried away by the undetected neutrinos. The backgrounds are due to leptonic decays of $W^+W^-$ pairs and other four fermion processes such as $e^+e^- \rightarrow W^+e^-\bar{\nu}$, two fermion processes ($f\bar{f}$), such as $e^+e^- \rightarrow q\bar{q}(\gamma)$ and $e^+e^- \rightarrow \tau^+\tau^-(\gamma)$, and two photon interactions ($\gamma\gamma$).

Events containing 2 to 6 charged particles of more than 400 MeV/$c$, with a total detected energy in the event not exceeding 0.45 $\sqrt{s}$ and a measured energy in charged particles greater than 0.04 $\sqrt{s}$ have been selected in the fully leptonic channel. In order to reject cosmic ray events, at least one of the charged particles has been required to have a distance in space within 0.2 cm from the position of the LEP colliding beam envelope. The energy detected within a cone of 30° half aperture around the beam axis had to be lower than 0.10 $\sqrt{s}$. The component of the total energy transverse to the beam axis had to be larger than 0.05 $\sqrt{s}$. After clustering the event into two jets by the DURHAM algorithm, the maximum angle between two particles within a jet had to be smaller than 30°, the angle between the beam axis and either jet and the angle between the two jets had to be larger than 20°.

In order to reject events fulfilling the above preselection cuts where the jets are back-to-back and radiative production of $Z^0$ events with a photon along the beam pipe, the following angular cuts have been applied. The angle between the projections of the jets on the plane perpendicular to the beam axis as well as the angle between the two jets must not exceed 167°.

The total energy of each of the two jets, $E_1$ and $E_2$, had to be greater than 0.02 $\sqrt{s}$. In addition the energy of the least energetic jet, $E_2$, was also required to be smaller than 0.13 $\sqrt{s}$ (see Figure 3).

Table 3: *Number of selected events and signal efficiency in the leptonic channel at different stages of the event selection for $\sqrt{s}$ = 183 GeV.*

| Selection | Data | Total Bkg | $W^+W^-$ Bkg | $ff$ Bkg | $\gamma\gamma$ Bkg | Efficiency $H^+H^-$ ($M_H$=60 GeV/$c^2$) |
|---|---|---|---|---|---|---|
| Event Preselection | 211 | 208.8 ± 3.6 | 26.0 | 160.0 | 22.8 | 0.45 ± 0.02 |
| Angular Cuts | 23 | 28.1 ± 1.0 | 24.9 | 0.8 | 2.4 | 0.44 ± 0.02 |
| Energy Cuts | 13 | 14.3 ± 0.6 | 13.1 | 0.1 | 1.1 | 0.32 ± 0.02 |

Due to the presence of the missing neutrinos in the decay of each of the two bosons, it is not possible to reconstruct the boson mass in the leptonic channel on an event-by-event basis and the signal corresponds to an inclusive excess of events compared to the expected backgrounds. The numbers of real data events, those from expected backgrounds and the signal efficiencies after each set of cuts adopted in the analysis are given in Table 3.

## 3 Results

### 3.1 Optimisation of the selection

The analysis applied at $\sqrt{s}$ = 183 GeV has been repeated for the data collected at $\sqrt{s}$ = 161 GeV and 172 GeV. After the event preselection procedure described above, the

separation of the candidate signal events from the backgrounds in the semi-leptonic and fully hadronic final states has been obtained by cuts on the two likelihoods characterising the probability for a given event to be due to either a $W^+W^-$ decay or a QCD process. The values of these cuts have been optimized by minimizing, on a sample of simulated events, the value of the $H^+H^-$ production cross-section that could be excluded with statistics equivalent to those of the real data. This minimization has been carried out simultaneously for the two probabilities. The correlations of the two probabilities for the background $W^+W^-$ and QCD samples, the $H^+H^-$ signal events and the real data are shown in Figure 1 and Figure 2 for the hadronic and semileptonic channels respectively.

Due to the differences in the integrated luminosity, $H^+H^-$ production cross-section and backgrounds, the final cuts on the likelihood variables for the hadronic and semileptonic channels were optimised independently at the different $\sqrt{s}$ energies.

These criteria have been applied to simulated signal $H^+H^-$ decays. The mass resolutions have been estimated to be 1.7 GeV/$c^2$ for the hadronic and 3.5 GeV/$c^2$ for the semileptonic channel. The number of real data and background events and the estimated efficiencies for these selections for different $H^\pm$ masses are summarised in Table 4 for the three final states.

Table 4: *Number of events, expected background and signal efficiencies for different charged Higgs masses in the hadronic, semileptonic and leptonic channels.*

| $\sqrt{s}$ | Channel | Data | Expected Bkg. | Eff. $M_H$ = 50 GeV/$c^2$ | Eff. $M_H$ = 55 GeV/$c^2$ | Eff. $M_H$ = 60 GeV/$c^2$ | Eff. $M_H$ = 65 GeV/$c^2$ |
|---|---|---|---|---|---|---|---|
| 161 | $c\bar{s}\bar{c}s$ | 8 | 5.3 ± 0.3 | 0.35 | 0.33 | 0.29 | 0.25 |
| 172 | $c\bar{s}\bar{c}s$ | 3 | 4.5 ± 0.3 | 0.31 | 0.30 | 0.29 | 0.29 |
| 183 | $c\bar{s}\bar{c}s$ | 11 | 11.8 ± 0.6 | 0.20 | 0.21 | 0.22 | 0.18 |
| 161 | $c\bar{s}\tau\bar{\nu}$ | 1 | 1.4 ± 0.2 | 0.40 | 0.39 | 0.37 | 0.35 |
| 172 | $c\bar{s}\tau\bar{\nu}$ | 2 | 2.0 ± 0.2 | 0.40 | 0.39 | 0.36 | 0.30 |
| 183 | $c\bar{s}\tau\bar{\nu}$ | 4 | 3.3 ± 0.3 | 0.37 | 0.35 | 0.31 | 0.26 |
| 161 | $\tau\bar{\nu}\tau\nu$ | 0 | 0.7 ± 0.1 | 0.31 | 0.32 | 0.33 | 0.34 |
| 172 | $\tau\bar{\nu}\tau\nu$ | 0 | 2.1 ± 0.1 | 0.29 | 0.32 | 0.35 | 0.40 |
| 183 | $\tau\bar{\nu}\tau\nu$ | 13 | 14.3 ± 0.6 | 0.29 | 0.30 | 0.32 | 0.34 |

## 3.2 Determination of the mass limit

No excess of events compared to the expected backgrounds has been observed in any of the three different final states investigated. A lower limit for a charged Higgs boson mass has been derived at the 95% confidence level as a function of the hadronic Higgs decay branching ratio BR(H $\rightarrow$ *hadrons*). The confidence in the signal hypothesis, $CL_s$, has been calculated using the likelihood ratio technique [15]. That is, first we find the ratio of the likelihood of the observed candidates, assuming signal plus background to that found using the background only hypothesis. The confidence levels $CL_{sb}$ and $CL_b$ are computed as the fractions of Gedanken experiments, with respectively signal plus background or background only, which gave likelihood ratio values smaller than those observed for the data. Finally we make the conservative step of defining $CL_s$ as the ratio of these probabilities: $CL_s = \frac{CL_{sb}}{CL_b}$.

The required Gedanken experiments have been made by Monte Carlo simulation, using the expected background and signal rates, as well as the background and signal probabil-

ity density functions of one discriminating variable in each channel. In the hadronic and semi-leptonic channels, the discriminating variable is the reconstructed mass while in the leptonic channel the energy of the most energetic jet has been used. The distributions for the discriminating variable of signal events, obtained by the simulation at different $H^{\pm}$ mass values for each $\sqrt{s}$, have been interpolated for intermediate mass values. The signal efficiencies have been fitted with polynomial functions, to obtain the expected signal rate at any given mass. Uncertainties in the expected background and in the signal efficiency have been accounted for. These uncertainties are due both to the finite simulation statistics available and to possible differences in the response of the selection variables in data and simulation. The background events in simulation have been reweighted such that each variable agreed in shape with that of the real data and the background has been recomputed. The overall background uncertainty has been obtained by summing in quadrature the differences in the background estimates, after changing each of the variables, and the statistical error. A Gaussian smearing of the central values of the number of expected background events by their estimated uncertainties has been introduced in the limit derivation program. The uncertainties on the signal efficiencies are dominated by their statistical errors and have also been accounted for. The results are summarised in Figure 4. Independent of the hadronic decay branching ratio, a lower $H^{\pm}$ mass limit of $M_{H^{\pm}} > 56.3$ GeV/$c^2$ can be set at the 95% confidence level. For fully leptonic decays of the charged Higgs boson the limit becomes $M_{H^{\pm}} > 65.1$ GeV/$c^2$.

# 4 Conclusion

A search for pair-produced charged Higgs bosons has been performed using the full statistics collected by DELPHI at LEP at $\sqrt{s}$ of 161 GeV, 172 GeV and 183 GeV. Candidate events have been searched for in the $\tau\bar{\nu}\tau\nu$, $c\bar{s}\tau\bar{\nu}$ and $c\bar{s}\bar{c}s$ final states. No significant excess of candidates has been observed and a lower limit on the charged Higgs mass of 56.3 GeV/$c^2$ has been set at the 95% confidence level.

## Acknowledgements

We are greatly indebted to our technical collaborators, to the members of the CERN-SL Division for the excellent performance of the LEP collider, and to the funding agencies for their support in building and operating the DELPHI detector.
We acknowledge in particular the support of
Austrian Federal Ministry of Science and Traffics, GZ 616.364/2-III/2a/98,
FNRS–FWO, Belgium,
FINEP, CNPq, CAPES, FUJB and FAPERJ, Brazil,
Czech Ministry of Industry and Trade, GA CR 202/96/0450 and GA AVCR A1010521,
Danish Natural Research Council,
Commission of the European Communities (DG XII),
Direction des Sciences de la Matière, CEA, France,
Bundesministerium für Bildung, Wissenschaft, Forschung und Technologie, Germany,
General Secretariat for Research and Technology, Greece,
National Science Foundation (NWO) and Foundation for Research on Matter (FOM), The Netherlands,
Norwegian Research Council,
State Committee for Scientific Research, Poland, 2P03B06015, 2P03B1116 and SPUB/P03/178/98,
JNICT–Junta Nacional de Investigação Científica e Tecnológica, Portugal,
Vedecka grantova agentura MS SR, Slovakia, Nr. 95/5195/134,
Ministry of Science and Technology of the Republic of Slovenia,
CICYT, Spain, AEN96–1661 and AEN96-1681,
The Swedish Natural Science Research Council,
Particle Physics and Astronomy Research Council, UK,
Department of Energy, USA, DE–FG02–94ER40817.

# References


[1] DELPHI Collaboration, P. Abreu *et al.*, *E. Phys. J.* **C 2** (1998), 1 and *Phys. Lett.* **B 420** (1998), 140.

[2] ALEPH Collaboration, R. Barate *et al.*, CERN-EP/99-011, submitted to *Phys. Lett.* **B**;
L3 Collaboration, M. Acciarri *et al.*, *Phys. Lett.* **B 446** (1999), 368;
OPAL Collaboration, G. Alexander *et al.*, *Phys. Lett.* **B 426** (1998), 180.

[3] DELPHI Collaboration, P. Aarnio *et al.*, *Nucl. Instr. and Meth.* **A 303** (1991), 223.

[4] DELPHI Collaboration, P. Abreu *et al.*, *Nucl. Instr. and Meth.* **A 378** (1996), 57.

[5] M. Battaglia and P.M. Kluit, *Particle Identification using the DELPHI RICH Detectors*, to appear in the *Proc. of the 3$^{rd}$ Int. Workshop on Ring Imaging Cherenkov Detectors, RICH 98*, *Nucl. Instr. and Meth.* **A** (1999).

[6] T. Sjöstrand, *Comp. Phys. Commun.* **82** (1994), 74.

[7] F.A. Berends, R. Pittau, R. Kleiss, *Comp. Phys. Commun.* **85** (1995), 437.

[8] S. Nova, S. Olshevski and T. Todorov, in Cern Report 96-01, Vol. II, 224.

[9] F.A. Berends, P.H. Daverveldt and R. Kleiss, *Comp. Phys. Commun.* **40** (1986), 271, 285 and 309.

[10] S. Jadach, B.F.L. Ward and Z. Was, *Comp. Phys. Commun* **79** (1994), 503.

[11] DELPHI Collaboration, P. Abreu *et al.*, CERN-EP/99-06, to be published in *E. Phys. J.* **C** (1999).

[12] A similar jet flavour tagging technique has been used in DELPHI Collaboration, P. Abreu *et al. Phys. Lett.* **B 439** (1998), 209.

[13] DELPHI Collaboration, P. Abreu *et al.*, *E. Phys. J.* **C 2** (1998), 581.

[14] S. Catani *et al. Phys. Lett.* **B 269** (1991), 432.

[15] A.L. Read, *Optimal statistical analysis of search results based on the likelihood ratio and its application to the search for the MSM Higgs boson at 161 and 172 GeV*, DELPHI 97-158 PHYS 737.

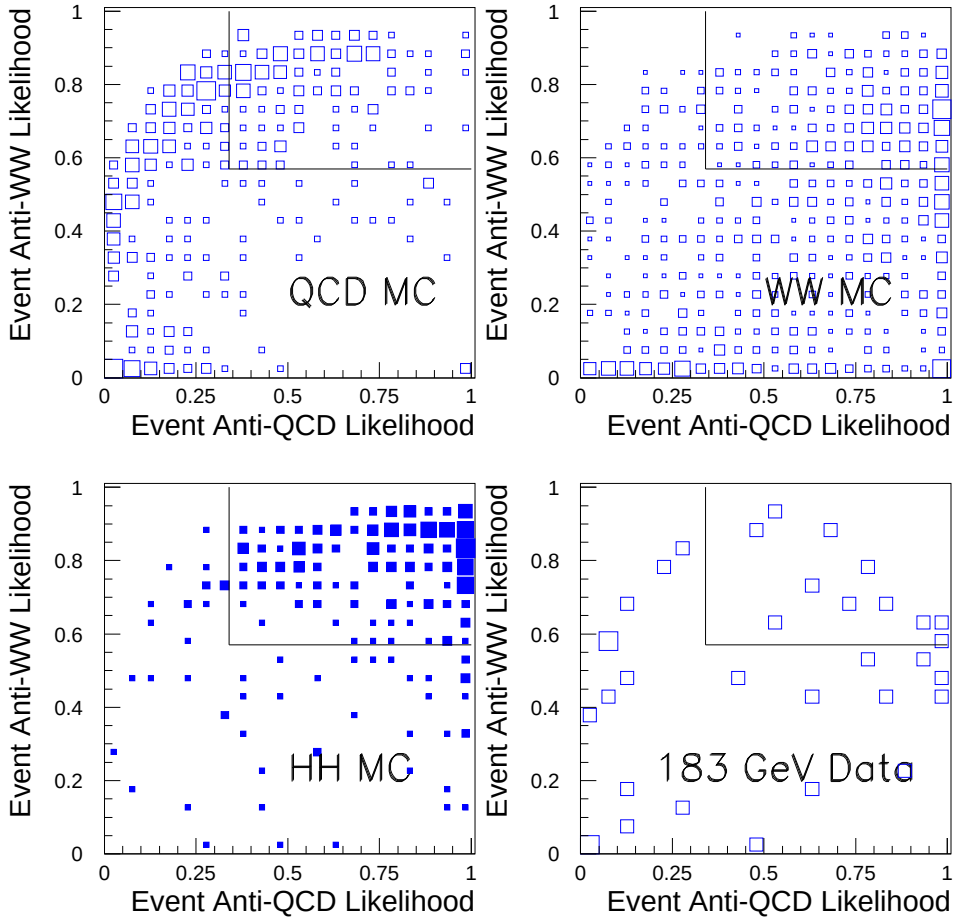


Figure 1: Correlation plots of the event anti-QCD and anti-WW likelihoods used to discriminate between signal $H^+H^-$ events and backgrounds for simulated QCD events (upper left), $W^+W^-$ events (upper right), signal $H^+H^-$ for $M_H = 60$ GeV/$c^2$ (lower left) and the $\sqrt{s} = 183$ GeV real data (lower right) in the hadronic channel. The box indicates the signal region used in the analysis.

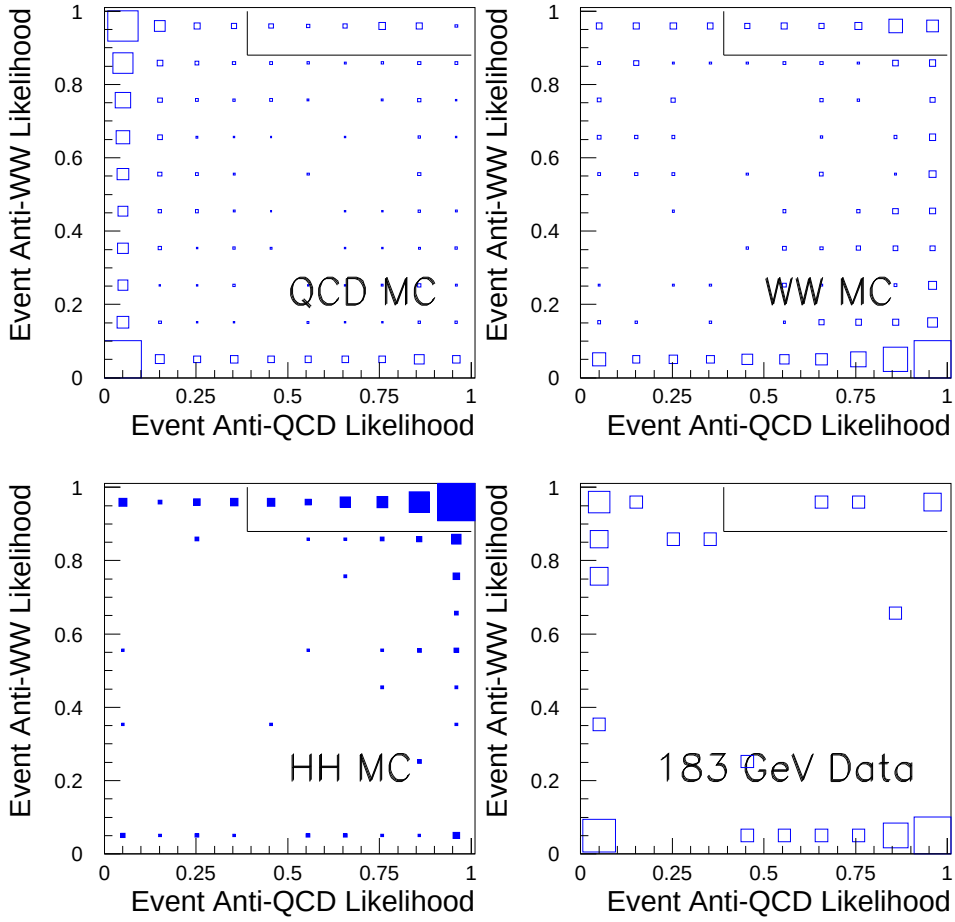


Figure 2: Correlation plots of the event anti-QCD and anti-WW likelihoods used to discriminate between signal $H^+H^-$ events and backgrounds for simulated QCD events (upper left), $W^+W^-$ events (upper right), signal $H^+H^-$ for $M_H = 60$ GeV/$c^2$ (lower left) and the $\sqrt{s} = 183$ GeV real data (lower right) in the semileptonic channel. The box indicates the signal region used in the analysis.

Figure 3: Correlation plots of the total energy fraction of the less energetic jet $E_2/\sqrt{s}$ vs. that for the more energetic jet $E_1/\sqrt{s}$ used to discriminate between the signal and the backgrounds in the fully leptonic channel for simulated $W^+W^-$ decays (upper left), $\gamma\gamma$ events (upper right), signal $H^+H^-$ for $M_H = 60$ GeV/$c^2$ (lower left) and the $\sqrt{s} = 183$ GeV real data (lower right). The lines show the cuts defining the signal region used in the analysis. The distribution of $E_1/\sqrt{s}$ for the selected events has been used as discriminating variable in the limit derivation program.

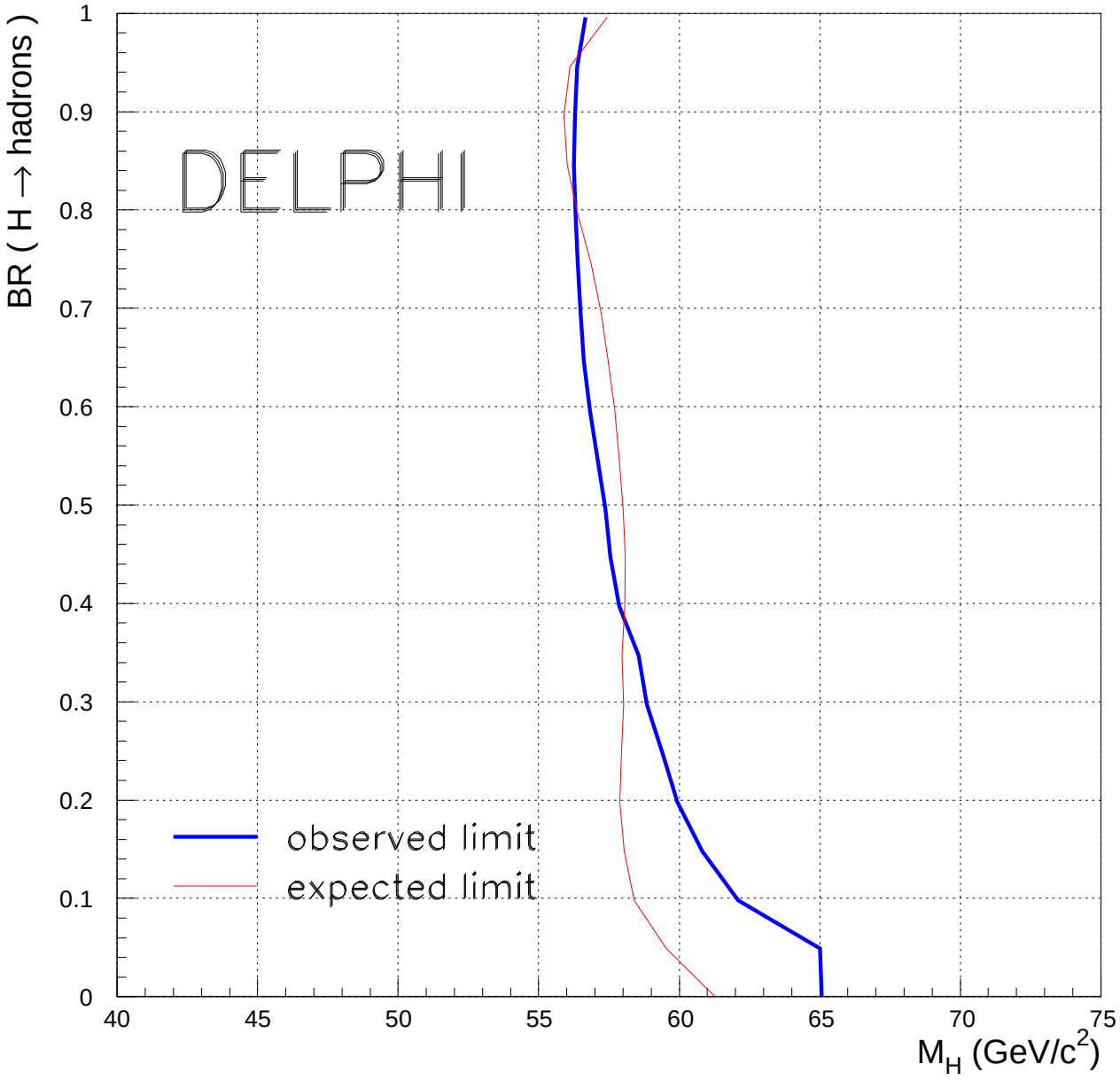


Figure 4: The 95% confidence level observed and expected exclusion regions for $H^{\pm}$ in the plane BR(H $\rightarrow$ hadrons) vs. $M_{H^{\pm}}$ obtained from a combination of the search results in the hadronic, semileptonic and fully leptonic decay channels at $\sqrt{s} = 161$ GeV, 172 GeV and 183 GeV. The sharp decrease at 65 GeV/$c^2$ in the leptonic channel reflects the maximum signal mass considered in the lower energy samples.